MSc Technical Medicine

Improved therapy planning for eye tumours: a tumour geometry comparison between MRI and conventional ultrasound

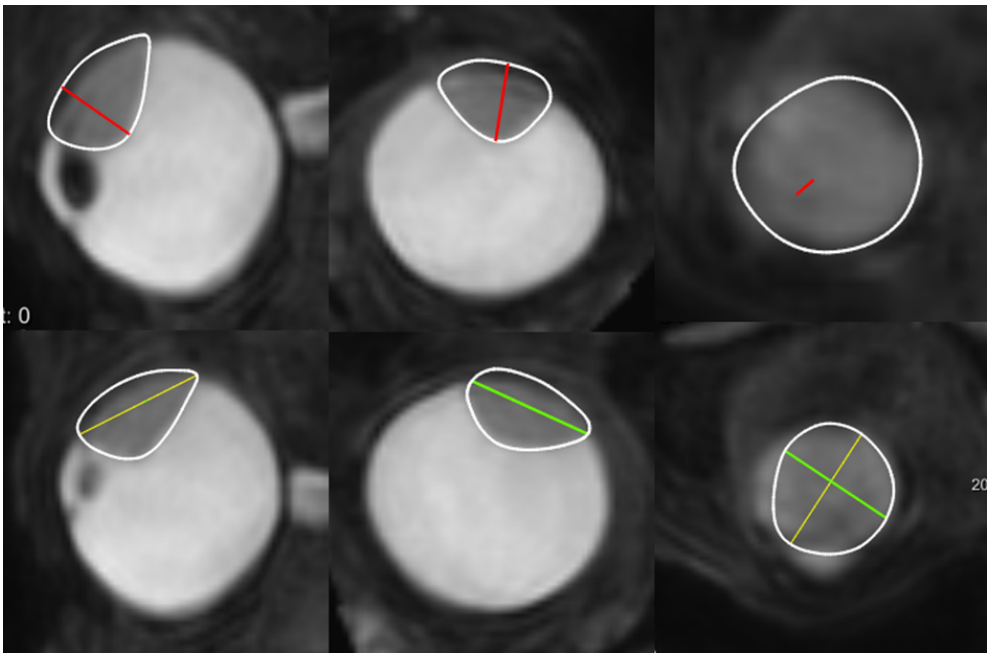

Student:
Lisa Klaassen

Supervision:
J-W.M. Beenakker
M.G. Jaarsma-Coes
G.P.M. Luyten

Leids Universitair Medisch Centrum

TU Delft Delft University of Technology

Erasmus MC Universitair Medisch Centrum Rotterdam

Contents

General information and abstract

Student: Lisa Klaassen
Student number: 4375327
Master programme: Technical Medicine
Track: Imaging and Interventions
Date: 03-11-2020
Defense date: 18-11-2020

Internship location: Departments of Ophthalmology and Radiology, LUMC
Medical supervision: Prof. dr. G.P.M. Luyten
Technical supervision: Dr. J-W.M. Beenakker
Daily supervision: M.G. Jaarsma-Coes, MSc

Improved therapy planning for eye tumours: a tumour geometry comparison between MRI and conventional ultrasound

Introduction: Uveal melanoma is the most frequently occurring primary eye tumour. The aim of this research was to determine the difference in geometrical tumour measurements between ultrasound and magnetic resonance imaging (MRI), to compare MRI and ultrasound-based tumour models, and to evaluate the clinical implications of these differences for uveal melanoma patients.
Methods: Tumours of 42 uveal melanoma patients were segmented on T2-weighted MRI scans. Prominence, largest basal diameter (LBD), and second basal diameter (SBD) were calculated automatically and compared to clinical ultrasound measurements. Volumes of segmented MRI tumours were compared to the volumes of ellipsoid ultrasound-based models.
Results: For the prominence, LBD, and SBD, the mean absolute differences were 0.8 ± 0.7 mm, 1.6 ± 1.3 mm and 1.6 ± 1.4 mm between the conventional ultrasound measurement and the MRI measurement. A significant difference was observed for the prominence between anteriorly and posteriorly located tumours (0.6 ± 0.5 mm versus 1.1 ± 0.8 mm, p = 0.02). Tumour volume on MRI was on average 70 mm^3 smaller than the ultrasound tumour model volume, with a dice similarity coefficient of 0.81 ± 0.10.
Conclusion: The largest clinical impact of the use of MRI measurements may be observed in tumours with a prominence between 6 and 8 mm and a LBD between 14 and 18 mm. Furthermore, the use of MRI could add valuable shape information to proton beam therapy planning.

Introduction

Uveal melanomas are the most frequently occurring primary eye tumour, with an incidence of about 6 per million in Europe and the USA [1]. They arise from melanocytes in the uveal tract, with about 85 % originating in the choroid, 5-8 % in the ciliary body and 3-5 % in the iris [1]. Clinical symptoms include blurred vision, light flashes or floaters, visual field loss, pain, and metamorphopsia. However, symptoms seldomly occur until the lesion is large, and about 30 % of patients are asymptomatic at diagnosis [2]. Therefore, diagnosis often follows routine check-ups or diabetic retinopathy screening. A combination of imaging modalities, such as indirect ophthalmoscopy, ultrasound, and optical coherence tomography can be used to confirm the diagnosis [2].

Clinical treatment decision making and radiotherapy planning for uveal melanoma rely mostly on ultrasound (US) measurements (Figure 1), such as tumour prominence (depth), largest basal diameter (LBD) and second basal diameter (SBD) [1, 2, 3]. A slight deviation in these measurements can result in a shift between an eye-preserving treatment, such as brachytherapy or proton beam therapy (PBT), and enucleation. In ruthenium brachytherapy, the LBD is used to determine the applicator providing the most optimal tumour coverage [4]. Furthermore, a correct prominence measurement is essential to ensure application of the prescribed tumour dose. In PBT, the prominence, LBD and SBD (measured perpendicularly to the LBD) are used to construct a tumour model for dose calculations and dose delivery planning [5]. However, this model is limited, as it is constructed based on 2D measurements of a 3D structure. Furthermore, these measurements itself are limited as well, as US is a 2D imaging technique. Moreover, for accurate geometrical tumour measurements the US transducer needs to be placed perpendicularly to the tumour, which can be impossible in particular cases due to the location of the tumour and structures around the eye.

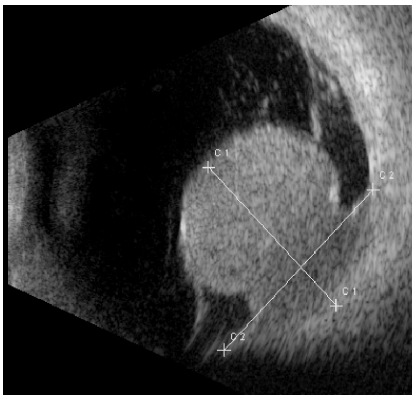

FIGURE 1: Example of a B-scan US of a mushroom-shaped uveal melanoma.

Recent advances have enabled high resolution magnetic resonance imaging (MRI) in a clinical setting, providing three-dimensional imaging of the tumour [6]. Previous studies have reported a median absolute difference in prominence of approximately 1 mm, when measured on US and MRI [7, 8]. In the study of Beenakker et al. [7], the difference between the measurements led to a switch in treatment in 2 out of 10 patients. However, this study had a limited range of tumour prominences. In the research performed in 2005 by Schueller et al. [8], measurements were performed on MRI scans with a slice thickness of 4 mm. All in all, a complete overview of the difference in prominence, LBD and SBD with contemporary techniques is lacking. Furthermore, with the introduction of ocular MRI, new opportunities arise to further implement 3D imaging techniques in PBT treatment planning [5, 9, 10]. For this purpose, knowledge of the difference between conventional tumour models and MRI tumour volume is crucial.

The aim of this study, therefore, was to determine the difference in geometrical tumour measurements between US and MRI, compare MRI and US-based tumour models, and to evaluate the clinical implications of these differences.

Methods

In this study, data of 42 patients was used. 34 patients were scanned after written informed consent as part of a prospective study approved by the local ethics committee. 3 patients with tumours originating in the iris or ciliary body were excluded for this study. The other 11 patients received an MRI as part of clinical care and their data was included retrospectively with approval of the local ethics committee.

Data acquisition

Patients were scanned in a 3 Tesla wide bore Philips Ingenia MRI-scanner (Philips Healthcare, Best, The Netherlands) with a 4.7 cm surface receive coil (Philips Healthcare, Best, The Netherlands) mounted on a flexible eye mask. For this study, the 3D Turbo-Spin Echo T2 scan (voxel size 0.8x0.8x0.8 mm^3, TE 293 ms, TR 2300 ms, Flip Angle 35 degrees, SPIR fat suppression) and the 3D Turbo-Spin Echo Gadolinium-enhanced T1 scan (voxel size 1.0x1.1x1.0 mm^3, TE 9.4 ms, TR 350 ms, SPIR fat suppression) were used (Figure 2). More details on scan set-up and sequences can be found in an earlier described ocular MRI protocol [6].

Tumour segmentation

After rigid registration of the 3D T2-weighted scan to the contrast-enhanced 3D T1-weighted scan, the tumours were segmented on the 3D T2-weighted scan in MeVisLab 3.0.2 (MeVis Medical Solutions AG, Bremen, Germany) [11], using Subdivision Surfaces controlled by the maximum gradient magnitude [12]. After automatic segmentation, manual adjustments were performed until consensus was reached between three observers. The sclera at the base of the tumour was considered to be a part of the tumour. The contrast-enhanced 3D T1-weighted scan was used to differentiate between tumour and retinal detachment and was used for segmentation when segmentation on the T2-weighted image not possible due to movement, which was the case in 6 patients.

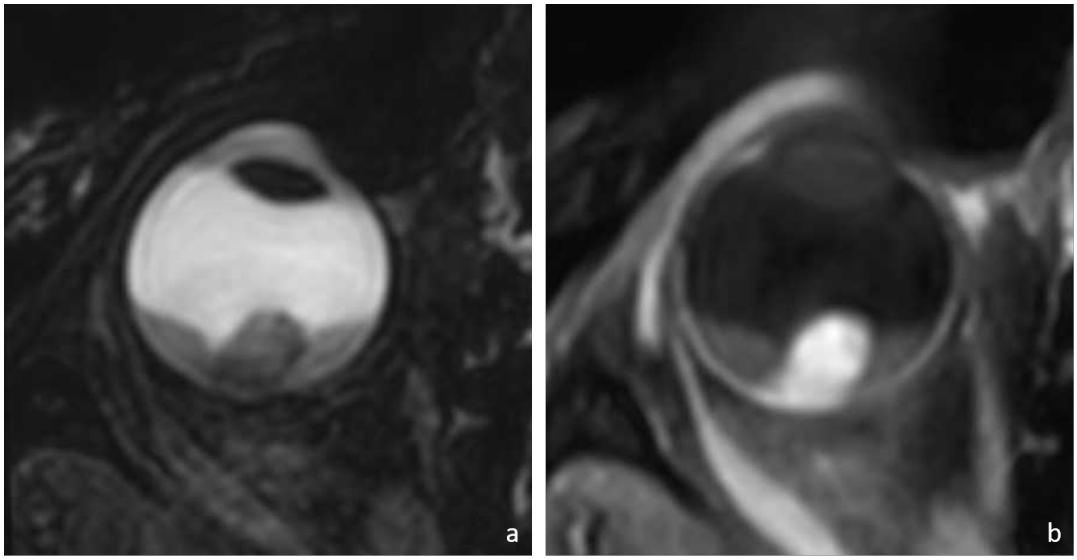

FIGURE 2: An example of (a) the 3D T2-weighted scan, (b) the contrast-enhanced 3D T1-weighted scan.

Geometrical tumour measurements

First, the prominence, LBD and SBD were calculated automatically based on the tumour segmentations. The prominence was defined as the maximum distance between the top and base of the tumour perpendicular to the sclera (± 5 degrees). The LBD was defined as the largest distance between two points in the base of the tumour and the SBD as the largest distance perpendicular to the LBD (± 5 degrees). An example of the automatic MRI measurements can be found in Figure 3.

Next, manual MRI measurements were performed in 3D reconstructions of the 3D T2-weighted scan by one experienced observer. Finally, the US measurements were performed as part of the regular care by an ophthalmologist.

Clinical usability of the automatic MRI measurements was assessed by an ophthalmologist on a scale from 1 (rejected) to 3 (clinically acceptable).

Subgroup analysis was performed for anterior versus superior tumour location, as for an anterior tumour location the correct placement of the US transducer is more difficult than for a posterior location. Patients who had tumours that were located neither anteriorly or posteriorly were not included in this analysis.

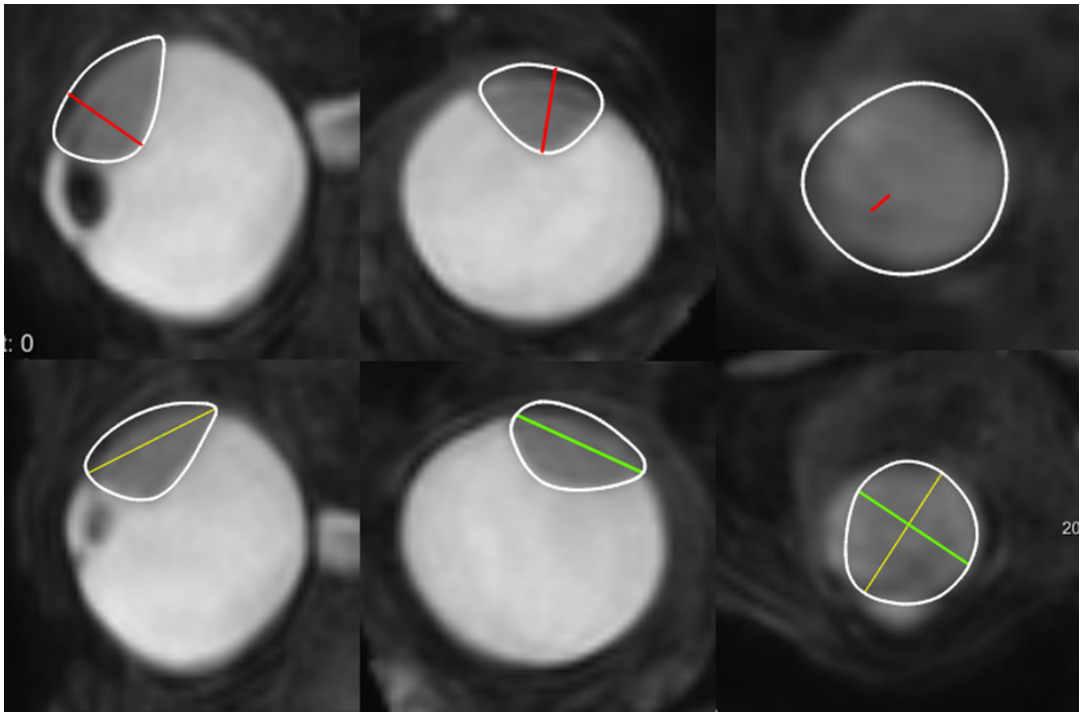

FIGURE 3: Automatic determination of tumour prominence (red), LBD (yellow) and SBD (green) on a 3D T2-weighted MRI scan.

Clinical impact

The difference in optimal treatment as determined by US and automatic MRI measurements was compared using the current clinical cut-off values as used at our centre (a prominence of 7 mm and a LBD of 16 mm).

3D tumour model

The volume of the US based tumour model (V_{US_model}), defined as an ellipsoid (Equation 1) [13, 14], was compared to the segmented MRI tumour (V_{MRI_tumour}), as shown in Figure 4. After iterative closest point registration, the volumes of overlap and non-overlap and the Dice Similarity Coefficient (DSC) (Equation 2) were computed. Two volumes of non-overlap were evaluated: $V_{US\_model-MRI\_tumour}$ (covered by the US model but not by the MRI tumour) and $V_{MRI\_tumour-US\_model}$ (covered by the tumour on MRI but not by the US model). Examples of the volumes of overlap and non-overlap are shown in Figure 5. To determine whether the volume differences found were caused by the shape difference between the US model and the MRI tumour or by the difference in geometrical tumour measurements, the analysis was repeated with the combination of an ellipsoid model based on the automatic MRI measurements (V_{MRI_model}) and the segmented MRI tumour (V_{MRI_tumour}).

$$V = \frac{\pi}{6} * prominence * LBD * SBD \tag{1}$$

$$DSC = \frac{2 * |V_{US\_model} \cap V_{MRI\_tumour}|}{|V_{US\_model}| + |V_{MRI\_tumour}|} \tag{2}$$

Statistical analysis

The means of the US and MRI measurement for the prominence, LBD and SBD were compared with MANOVA test with a Tukey HSD post-hoc analysis. The tumour position analysis was performed with an independent T-test and the difference between V_{MRI_tumour} and V_{US_model} was analysed with a paired samples T-test. For all tests, significance was assumed at $\alpha < 0.05$.

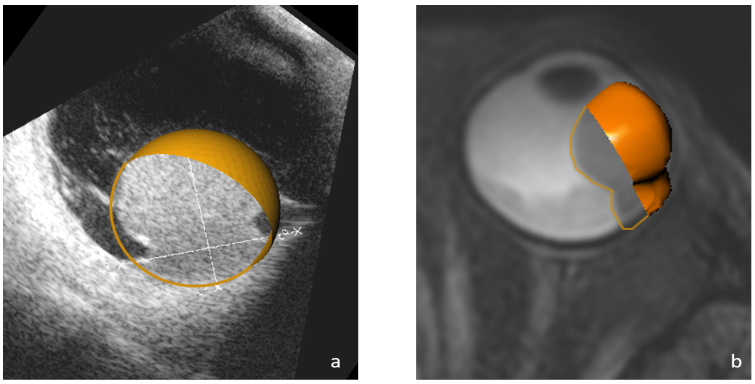

FIGURE 4: (a) a uveal melanoma on US, with its US tumour model, (b) the same uveal melanoma on MRI with its segmented tumour.

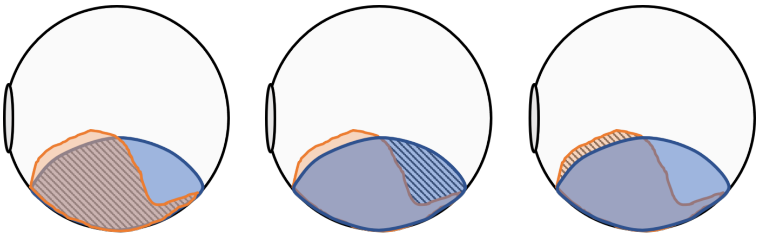

FIGURE 5: Examples of the volumes of overlap and non-overlap (striped) for the US model (blue) and the segmented tumour on MRI (orange). (a) Volume of overlap, (b) volume of non-overlap $V_{US\_model-MRI\_tumour}$, (c) volume of non-overlap $V_{MRI\_tumour-US\_model}$

Results

Population

Subjects were 65 ± 12 years old and 76 % of subjects were male. 50 % of the patients underwent ruthenium brachytherapy, while 36 % received PBT and 14% underwent enucleation. Tumours were located as follows: 38 % anterior, 50 % posterior, and 12 % undefined. 71 % of tumours was dome shaped, while mushroom shaped and irregularly shaped tumours both accounted for 14 % of tumours. 68 % of tumours were melanotic, 13 % were amelanotic and 19 % was mixed.

Measurement quality

Clinical acceptability was assessed by an ophthalmologist for the automatic MRI measurements. For the prominence measurements, 29 out of 42 measurements were clinically acceptable, while 7 measurements were debatable and 6 measurements were rejected. All rejected measurements were large tumours (prominence >10 mm on US) and were rejected because the base coordinates of the calculated prominence were located too far from the centre of the base to accurately represent the clinical prominence measurement. Examples of clinically acceptable, debatable and rejected automatic prominence measurements can be found in Appendix 1. For the LBD, 40 out of 42 measurements were clinically acceptable, while 2 measurements were rejected. For the SBD, 39 out of 42 measurements were clinically acceptable, with 2 measurements debatable and 1 measurement rejected. Rejected and debatable measurements are marked in Figures 6, 7 and 8.

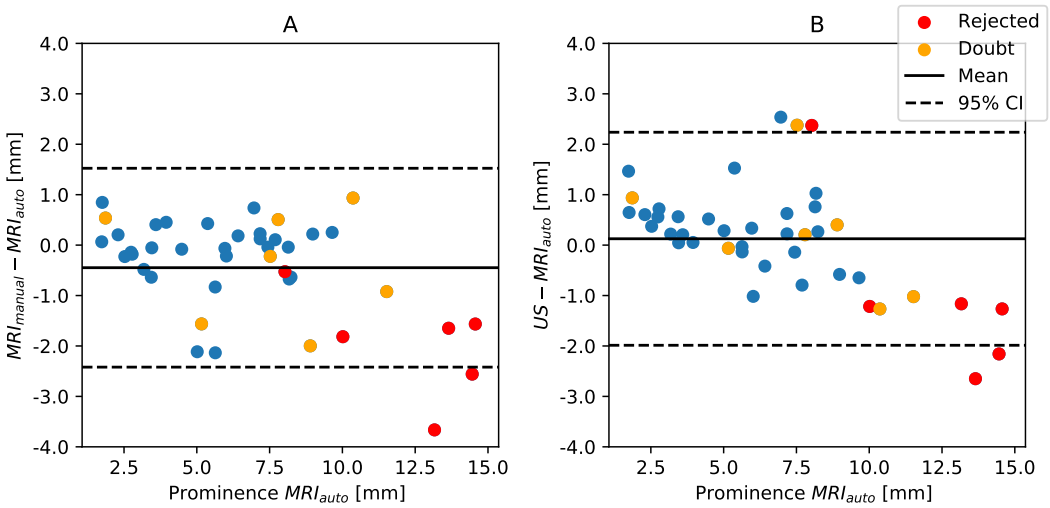

FIGURE 6: (A) The difference between the automatic and manual MRI measurements for the prominence, (B) the difference between the US measurement and the automatic MRI measurement for the prominence. Rejected and debatable measurements are shown in orange and red.

Geometrical tumour measurements

First, the automatic MRI measurements were compared to the manual MRI measurements (Figures 6a, 7a, and 8a, Table 1). Mean absolute differences for the automatic versus manual measurements were 0.8 ± 0.8 mm for the prominence, 2.6 ± 1.8 mm for the LBD and 1.5 ± 1.2 mm for the SBD, respectively. The manual LBD measurement was on average almost 2 mm smaller than the automatic measurement (Figure 7a). Since almost all of the automatic

LBD measurements were clinically acceptable, we assume the manual MRI measurement underestimates the true LBD. Therefore, in the rest of the analyses in this section, the automatic MRI measurements were used.

No significant differences were found between the means of the geometrical tumour measurements for the three measurement methods (Table 1, Appendix 2). However, for individual patients, the absolute differences between the US and MRI measurements varied. To illustrate this, the mean absolute differences between the three measurement methods were reported as well (Table 1, Figures 6b, 7b, and 8b).

For the prominence, a mean absolute difference of 0.8 ± 0.7 mm was observed (Figure 6b). For three patients, the prominence was more than 2 mm larger on the US measurement. For these patients, the tumour was located anteriorly and for one patient, the automatic MRI measurement was rejected. In a group of seven patients, the prominence measured on MRI was larger than 10 mm, whereas the prominence on US was at least 1 mm smaller. However, the automatic MRI measurement was rejected or debatable for these patients. When the rejected measurements were left out of the analysis, the mean absolute difference for the prominence was 0.7 ± 0.6 mm.

	Value		**Absolute difference w.r.t. US measurement**		**Absolute difference w.r.t. manual MRI measurement**	
	Mean [mm]	SD [mm]	Mean [mm]	SD [mm]	Mean [mm]	SD [mm]
Prominence						
US measurement	6.85	2.95	-	-	0.98	0.77
MRI automatic	6.71	3.52	0.79	0.67	0.76	0.83
MRI manual	6.28	3.05	0.98	0.77	-	-
LBD						
US measurement	13.66	3.17	-	-	2.11	1.53
MRI automatic	14.36	3.93	1.56	1.33	2.63	1.75
MRI manual	12.07	3.26	2.11	1.53	-	-
SBD						
US measurement	11.39	2.68	-	-	1.80	1.63
MRI automatic	10.84	2.92	1.58	1.38	1.48	1.24
MRI manual	10.66	3.20	1.80	1.63	-	-

TABLE 1: Mean values with standard deviations and absolute differences for all measurement methods.

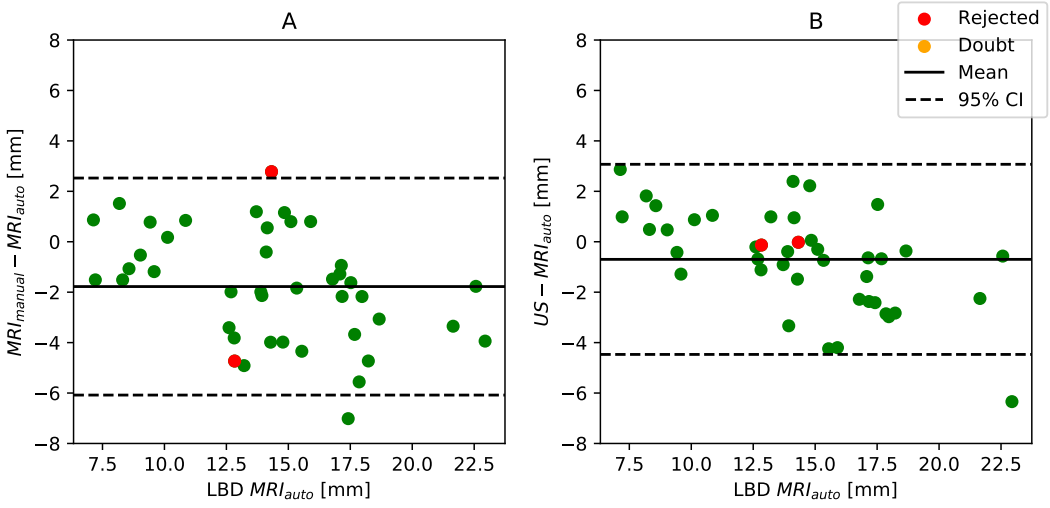

FIGURE 7: The difference between measurement methods for the LBD. Rejected and debatable measurements are shown in orange and red.

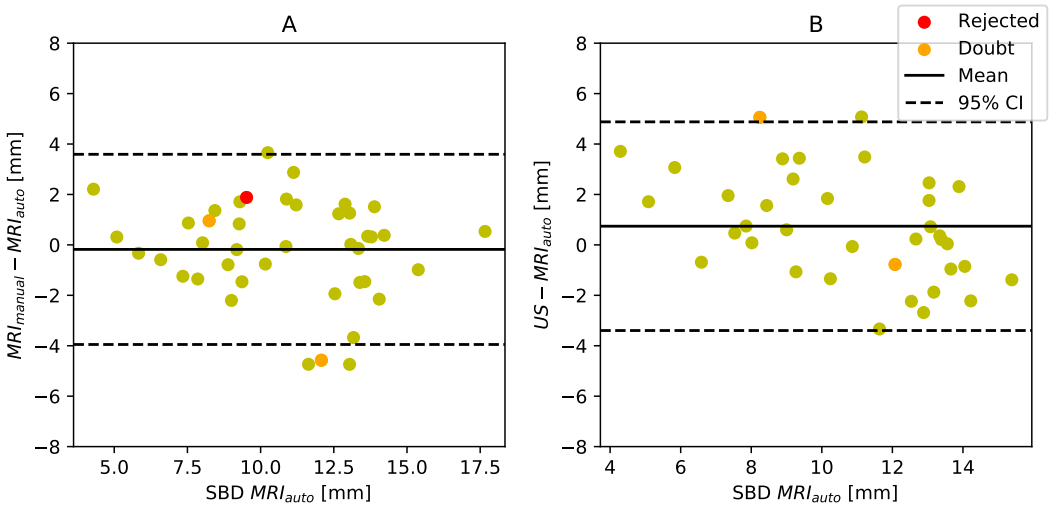

FIGURE 8: The difference between measurement methods for the SBD. Rejected and debatable measurements are shown in orange and red.

For the LBD, a mean absolute difference of 1.6 ± 1.3 mm was found (Figure 7b). Here, the automatic MRI measurements were often larger than the US measurements, with two outliers at -4.2 mm and -6.3 mm. Both tumours were located temporally. Furthermore, one of these tumours had a flat extension at the base, which may not have been considered part of the tumour in the US measurement. Due to the differences in LBD, 3 out of 42 patients would shift in treatment from ruthenium to PBT/enucleation. Furthermore, 5 patients became eligible for a different brachytherapy plaque size: 3 patients could possibly receive a smaller plaque, while 2 needed a larger plaque.

The SBD had a mean absolute difference of 1.6 ± 1.4 mm (Figure 8b). The intersection between the LBD and SBD was located 0.6 % to 38.0 % away from the middle of the LBD, with an average of 14 %.

Effect of tumour location

Subgroup analysis was performed for tumour location in the anteroposterior direction. Only the prominence between the anterior and posterior tumours differed significantly, with mean absolute differences of 1.1 ± 0.8 mm and 0.6 ± 0.5 mm, respectively (p=0.02). When the rejected prominence differences were left out, mean absolute differences of 0.8 ± 0.2 mm for anteriorly located tumours and 0.3 ± 0.1 mm for posteriorly located tumours were measured (p=0.03). Complete results of the tumour location analysis are shown in Appendix 3.

3D tumour model

Mean volumes for the US tumour model and for the tumours on MRI were 597 ± 409 mm^3 and 527 ± 388 mm^3, respectively (p=0.03). The US model was larger than the MRI tumour in 77 % of cases.

The volume of overlap (Figure 9a) after registration was 467 ± 325 mm^3 and the corresponding DSC was 0.81 ± 0.10. The volumes of non-overlap, $V_{US\_model-MRI\_tumour}$ (Figure 9b) and $V_{MRI\_tumour-US\_model}$ (Figure 9c), were 129 ± 160 mm^3 (39 ± 41 % of V_{MRI_tumour}) and 60 ± 77 mm^3 (9 ± 8 % of V_{MRI_tumour}).

To determine whether the aforementioned volume differences were caused by the shape difference between the US model and the MRI tumour or by the difference in geometrical

tumour measurements only, the volumes V_{MRI_tumour} and V_{MRI_model} were compared. For these volumes, the volume of overlap was 536 ± 438 mm^3, with a DSC of 0.86 ± 0.06. The volumes of non-overlap, $V_{MRI\_model-MRI\_tumour}$ and $V_{MRI\_tumour-MRI\_model}$, were 122 ± 108 mm^3 and 45 ± 54 mm^3.

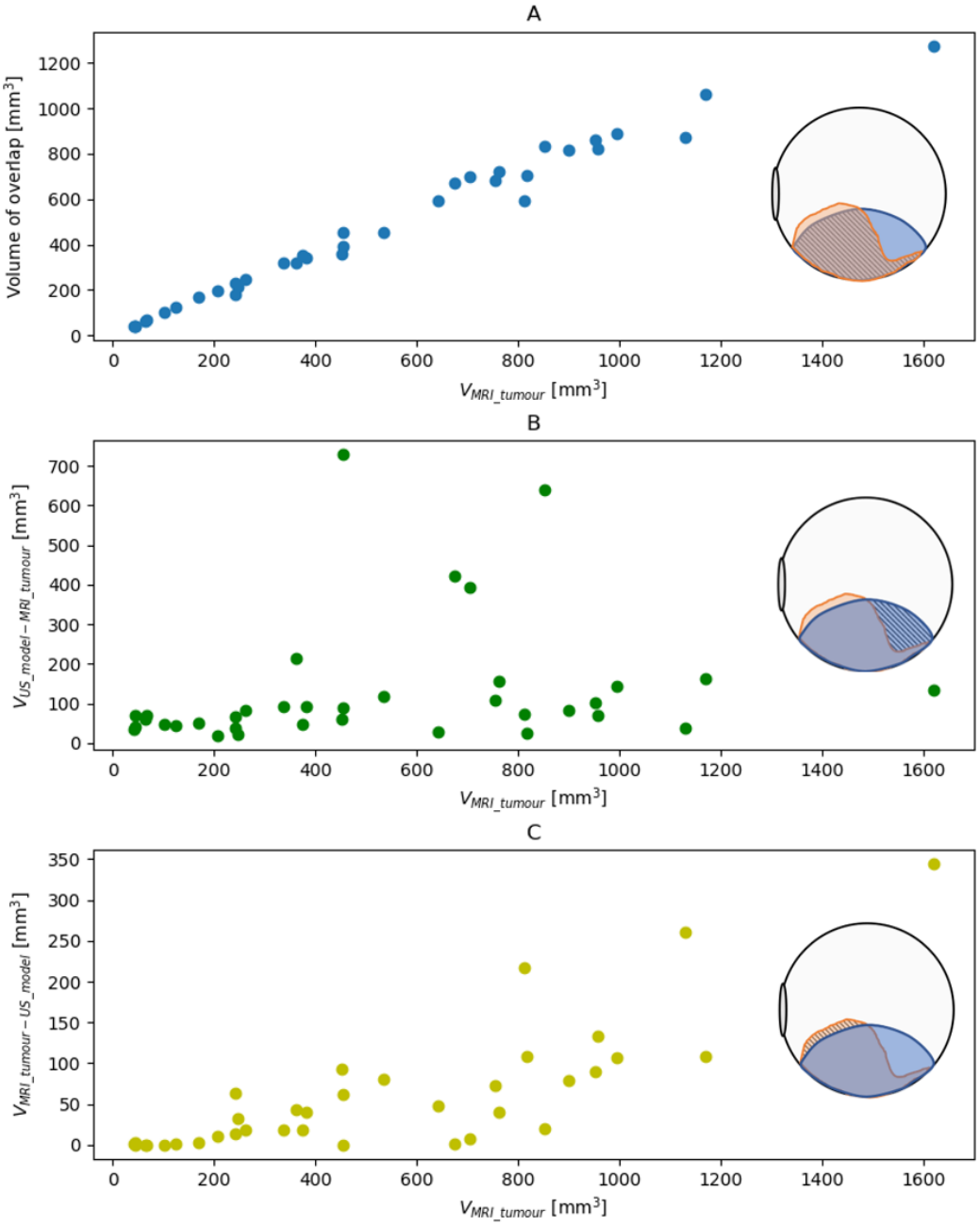

FIGURE 9: (a) Volume of overlap, (b) volume of non-overlap $V_{US\_model-MRI\_tumour}$, (c) volume of non-overlap $V_{MRI\_tumour-US\_model}$

Discussion

Geometrical tumour measurements, such as prominence, LBD and SBD, are the most important factor in treatment decision making for uveal melanomas. In this study, the use of MRI to measure these geometrical tumour measurements and tumour volume was compared to the conventional US measurements in a wide range of uveal melanoma patients: our cohort consisted of melanotic, amelanotic and mixed tumours, in a wide range of tumour sizes, with patients undergoing ruthenium brachytherapy, PBT, or enucleation.

The geometrical tumour measurements were evaluated manually and automatically on the MRI-scans, because manual measurements are quicker than the automatic measurements and are, therefore, more applicable in daily clinical practice, while automatic measurements suffer less from intra- and interobserver variability. We found a systematic underestimation of almost 2 mm when the LBD was measured manually. This indicates that it is difficult to manually determine the optimal measurement plane for the LBD, which was also reported by the observer performing the manual measurements.The automatic measurement, on the other hand, calculates all possibilities and will, therefore, always find the largest diameter.

For the automatic prominence measurements, a mean absolute difference of 0.8 mm was found between the conventional US measurement and the automatic MRI measurement. This corresponds to values found in literature [7, 8]. An overestimation of tumour prominence on US can partly be explained by an oblique cut through the tumour, especially for anteriorly located tumours, since it is more difficult to correctly position the US transducer. In this study, we observed a mean difference of 1.1 ± 0.8 mm in anteriorly located tumours, whereas posteriorly located tumours had a mean difference of 0.6 ± 0.5 mm (p=0.02). The differences found between US and MRI could also be caused by the better soft tissue contrast that MRI provides, resulting in a clearer distinction between tumour, retinal detachment, sclera, and orbital fat [7, 15].

Furthermore, in the evaluation of our automatic measurements, we noticed a lack of a clear definition of tumour prominence across ophthalmologists, radiologists and radiotherapists. At the beginning of this research, we defined the prominence as the maximum distance between the top and base of the tumour perpendicular to the sclera. In the evaluation of our automatic measurements, the scoring ophthalmologist rejected some measurements, that did meet this definition (Figure 10). With treatment planning becoming more precise, a need for a more precise prominence measurement exists. This can only be achieved if a consensus exist across disciplines. Possibly several different definitions could serve different goals, as the dose distributions and treatment planning for brachytherapy and PBT differ as well.

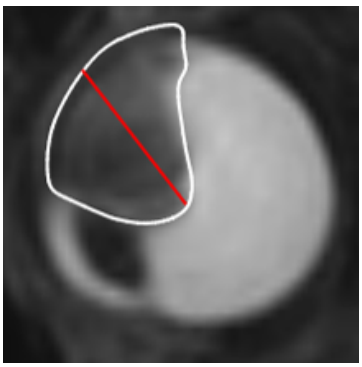

FIGURE 10: Example of rejected automatic prominence measurement.

For the LBD and SBD, the mean absolute differences between the US measurement and automatic MRI measurement were 1.6 ± 1.3 mm and 1.6 ± 1.4 mm. To our knowledge, this study is the first to compare LBD and SBD measurements between ultrasound and MRI. The differences found could have several causes: underestimation of these diameters on US can be caused by the difficulty in finding the correct measurement plane or the better soft tissue contrast on MRI mentioned earlier. On the other hand, an underestimation of tumour diameter can occur on MRI in flat melanomas and tumours with flat extensions [16]. Furthermore, inflammation at the edges of the tumour can be interpreted as tumour tissue on MRI, resulting in an overestimation of the tumour base.

Based on the automatic MRI measurements in this study, 3 out of 42 subjects would be eligible for a different treatment and 5 out of 42 for a different brachytherapy applicator size. This is less than the 20 % found by Beenakker et al. [7], which can be explained by the difference in sample: in this study, patients had a wider range of prominences. While treatment decision making would not solely be based on one modality in clinical practice, the mean differences observed in this study could be reason to prefer one treatment above another. This is especially the case for anteriorly located tumours and tumours with a prominence between 6 and 8 mm and/or a LBD between 14 and 18 mm, since these are close to the clinical cut-off values for treatment decision making at our centre.

In this study, we found that the tumour volume on MRI was on average 70 mm^3 smaller than the US tumour model volume, with a DSC of 0.81 ± 0.10. Via et al. [10] reach slightly smaller DSC values of 0.61 and 0.74 by two different observers, using a slightly different US model. The volume differences found in this study are larger than the differences found by Daftari et al. [17] (volume ratios between 0.993 and 1.02), but smaller than the volume reduction up to a factor 2, as reported by Marnitz et al [5]. In the study performed by Marnitz et al., a difference in tumour volume was also found between delineation on T2- and T1-weighted MRI-scans. In this study, delineation was performed on the T2-weighted scan, but the contrast-enhanced T1-weighted scan was used in case of uncertainty. We tried to address interobserver variabilities by using a semi-automated segmentation method and manually adjusting the contours with three observers.

The volumes of non-overlap (V_{US-MRI} and V_{MRI-US}) were 39 ± 41 % and 9 ± 8 % of the V_{MRI}, respectively. This could be considered an overestimation (V_{US-MRI}) and underestimation (V_{MRI-US}) of the true volume. Since, however, only a limited set of ruthenium brachytherapy applicators are available and no dose calculations were performed in this study, the exact clinical implications of the difference in tumour shape warrant further research. Some studies performed comparable analyses: Studenski et al. [13] found a small but significant difference in mean tumour dose and doses on several organs at risk when performing ruthenium brachytherapy planning on a true model based instead of a simplified ellipsoid model (but did not use the exact 3D tumour volume) and Tien et al. [14], comparing an ellipsoid model to a patient-specific CT-model for planning of iodine brachytherapy, observed a mean overprediction of 5.9 % for the target volume receiving the prescription dose. While some radiation of healthy tissue may be unavoidable due to the round shape of the plaques and homogenous distribution of the radiation source onto the ruthenium plaque surface [18], this is currently minimised by choosing the smallest brachytherapy applicator possible. With this study, we have shown that performing additional MRI scans in threshold cases or anteriorly located tumours may contribute to choosing the most suitable brachytherapy applicator.

In PBT, the dose distribution can theoretically be tailored more to each individual tumour shape, compared to brachytherapy. However, treatment planning is currently still mostly performed with a scaled geometric model of the eye [16]. We showed that the DSC between a MRI-based ellipsoid tumour model and the true tumour was 0.86 ± 0.06, indicating that the difference in geometrical tumour measurements between US and MRI cannot entirely explain the volumes of non-overlap between the US model and the segmented tumour on MRI. Therefore, MRI could contribute to a more precise description of tumour shape. While the construction of patient-specific MRI-based 3D eye models has already been shown feasible, integration with treatment planning systems has not been performed up to this point [16, 19, 20]. This study shows that the true tumour shape on MRI differs from ellipsoid US-based tumour models and illustrates the need for such an integration.

Limitations

A limitation of this study is the fact that 6 out of 42 (14 %) automatic prominence measurements were not clinically acceptable. In the evaluation of our automatic measurements, we noticed differences in interpretation between disciplines. Therefore, it would be necessary

to first reach a consensus across departments on the exact definition of the prominence, before improving the automatic calculation of the prominence. For now, the current automatic prominence calculation should not be applied to tumours with a prominence larger than 10 mm on US. Furthermore, no treatment planning comparison was performed on the MRI tumours versus the ultrasound models in this research. Therefore, the dosimetric effects of adding 3D tumour shape information to treatment planning are still unknown.

Conclusion

In this study, the use of MRI to measure prominence, LBD, SBD and tumour volume for uveal melanoma patients was compared to the conventional ultrasound methods. The largest differences were found for anteriorly located tumours. The largest clinical impact of the use of MRI measurements may be present in tumours with a prominence between 6 and 8 mm and LBD between 14 and 18 mm, due to the clinical cut-off point for treatment decision making. In conclusion, the use of MRI could add valuable shape information to PBT planning.

Acknowledgements

Firstly, I would like to thank Jan-Willem Beenakker, Myriam Jaarsma and professor Luyten for being my supervisors during this project. With every meeting, the end result became a little better and I appreciate everything you did for me in the past year. From the department of Ophthalmology, I would like to thank dr. Vu for the clinical evaluation of our automatic measurements and dr. Marinkovic for her opinions on both the literature review and some practical parts of this thesis. From the department of Radiotherapy, my thanks go to Martijn Ketelaars, for helping me understand more about brachytherapy for uveal melanoma and his advice in our meetings. Last but not least, working from home would have been a lot worse without the great people in the MReye group. Thank you for all the fun and also for your advice during our monday morning meetings.

Bibliography

[1] M. J. Jager, C. L. Shields, C. M. Cebulla, M. H. Abdel-Rahman, H. E. Grossniklaus, M. H. Stern, R. D. Carvajal, R. N. Belfort, R. Jia, J. A. Shields, and B. E. Damato. Uveal melanoma. *Nat Rev Dis Primers*, 6(1):24, 2020. doi: 10.1038/s41572-020-0158-0.

[2] S. Kaliki and C. L. Shields. Uveal melanoma: relatively rare but deadly cancer. *Eye (Lond)*, 31(2):241–257, 2017. doi: 10.1038/eye.2016.275.

[3] J. Yang, D. K. Manson, B. P. Marr, and R. D. Carvajal. Treatment of uveal melanoma: where are we now? *Ther Adv Med Oncol*, 10:1758834018757175, 2018. doi: 10.1177/1758834018757175.

[4] B. Damato, I. Patel, I. R. Campbell, H. M. Mayles, and R. D. Errington. Local tumor control after 106ru brachytherapy of choroidal melanoma. *Int J Radiat Oncol Biol Phys*, 63(2):385–91, 2005. doi: 10.1016/j.ijrobp.2005.02.017.

[5] S. Marnitz, D. Cordini, R. Bendl, A. J. Lemke, J. Heufelder, I. Simiantonakis, H. Kluge, N. E. Bechrakis, M. H. Foerster, and W. Hinkelbein. Proton therapy of uveal melanomas: intercomparison of mri-based and conventional treatment planning. *Strahlenther Onkol*, 182(7):395–9, 2006. doi: 10.1007/s00066-006-1512-1.

[6] T. A. Ferreira, L. Grech Fonk, M. G. Jaarsma-Coes, G. G. R. van Haren, M. Marinkovic, and J. M. Beenakker. Mri of uveal melanoma. *Cancers (Basel)*, 11(3), 2019. doi: 10.3390/cancers11030377.

[7] J. W. Beenakker, T. A. Ferreira, K. P. Soemarwoto, S. W. Genders, W. M. Teeuwisse, A. G. Webb, and G. P. Luyten. Clinical evaluation of ultra-high-field mri for three-dimensional visualisation of tumour size in uveal melanoma patients, with direct relevance to treatment planning. *MAGMA*, 29(3):571–7, 2016. doi: 10.1007/s10334-016-0529-4.

[8] P. Schueller, A. Dogan, J. E. Panke, O. Micke, and N. Willich. Does the imaging method have an influence on the measured tumor height in ruthenium plaque therapy of uveal melanoma? *Strahlenther Onkol*, 181(5):320–5, 2005. doi: 10.1007/s00066-005-1342-6.

[9] K. K. Mishra and I. K. Daftari. Proton therapy for the management of uveal melanoma and other ocular tumors. *Chin Clin Oncol*, 5(4):50, 2016. doi: 10.21037/cco.2016.07.06.

[10] R. Via, F. Hennings, A. Pica, G. Fattori, J. Beer, M. Peroni, G. Baroni, A. Lomax, D. C. Weber, and J. Hrbacek. Potential and pitfalls of 1.5t mri imaging for target volume definition in ocular proton therapy. *Radiother Oncol*, 154:53–59, 2020. doi: 10.1016/j.radonc.2020.08.023.

[11] F. Ritter, T. Boskamp, A. Homeyer, H. Laue, M. Schwier, F. Link, and H. O. Peitgen. Medical image analysis. *IEEE Pulse*, 2(6):60–70, 2011. doi: 10.1109/MPUL.2011.942929.

[12] P. H. Kitslaar, R. van 't Klooster, M. Staring, B. P. F. Lelieveldt, and R. J. van der Geest. Segmentation of branching vascular structures using adaptive subdivision surface fitting. *Medical Imaging 2015: Image Processing*, 9413, 2015. doi: Artn94133z10.1117/12.2082222.

[13] M. T. Studenski, N. V. Patel, A. Markoe, J. W. Harbour, and S. E. Samuels. Influence of tumor shape and location in eye plaque brachytherapy dosimetry. *Brachytherapy*, 19(2):249–254, 2020. doi: 10.1016/j.brachy.2020.01.001.

[14] C. J. Tien, M. A. Astrahan, J. M. Kim, M. Materin, Z. Chen, R. Nath, and W. Liu. Incorporating patient-specific ct-based ophthalmic anatomy in modeling iodine-125 eye plaque brachytherapy dose distributions. *Brachytherapy*, 16(5):1057–1064, 2017. doi: 10.1016/j.brachy.2017.06.014.

[15] L. Grech Fonk, T. A. Ferreira, A. G. Webb, G. P. M. Luyten, and J. M. Beenakker. The economic value of mr-imaging for uveal melanoma. *Clin Ophthalmol*, 14:1135–1143, 2020. doi: 10.2147/OPTH.S238405.

[16] J. Hrbacek, K. K. Mishra, A. Kacperek, R. Dendale, C. Nauraye, M. Auger, J. Herault, I. K. Daftari, A. V. Trofimov, H. A. Shih, Y. E. Chen, A. Denker, J. Heufelder, T. Horwacik, J. Swakon, C. Hoehr, C. Duzenli, A. Pica, F. Goudjil, A. Mazal, J. Thariat, and D. C. Weber. Practice patterns analysis of ocular proton therapy centers: The international optic survey. *Int J Radiat Oncol Biol Phys*, 95(1):336–343, 2016. doi: 10.1016/j.ijrobp.2016.01.040.

[17] Ik Daftari, E. Aghaian, J. M. O'Brien, W. Dillon, and T. L. Phillips. 3d mri-based tumor delineation of ocular melanoma and its comparison with conventional techniques. *Med Phys*, 32(11):3355–62, 2005. doi: 10.1118/1.2068927.

[18] F. J. Zaragoza, M. Eichmann, D. Fluhs, W. Sauerwein, and L. Brualla. Monte carlo estimation of absorbed dose distributions obtained from heterogeneous (106)ru eye plaques. *Ocul Oncol Pathol*, 3(3):204–209, 2017. doi: 10.1159/000456717.

[19] H. G. Nguyen, R. Sznitman, P. Maeder, A. Schalenbourg, M. Peroni, J. Hrbacek, D. C. Weber, A. Pica, and M. Bach Cuadra. Personalized anatomic eye model from t1-weighted volume interpolated gradient echo magnetic resonance imaging of patients with uveal melanoma. *Int J Radiat Oncol Biol Phys*, 102(4):813–820, 2018. doi: 10.1016/j.ijrobp.2018.05.004.

[20] C. Ciller, S. De Zanet, K. Kamnitsas, P. Maeder, B. Glocker, F. L. Munier, D. Rueckert, J. P. Thiran, M. Bach Cuadra, and R. Sznitman. Multi-channel mri segmentation of eye structures and tumors using patient-specific features. *PLoS One*, 12(3):e0173900, 2017. doi: 10.1371/journal.pone.0173900.

Appendix 1

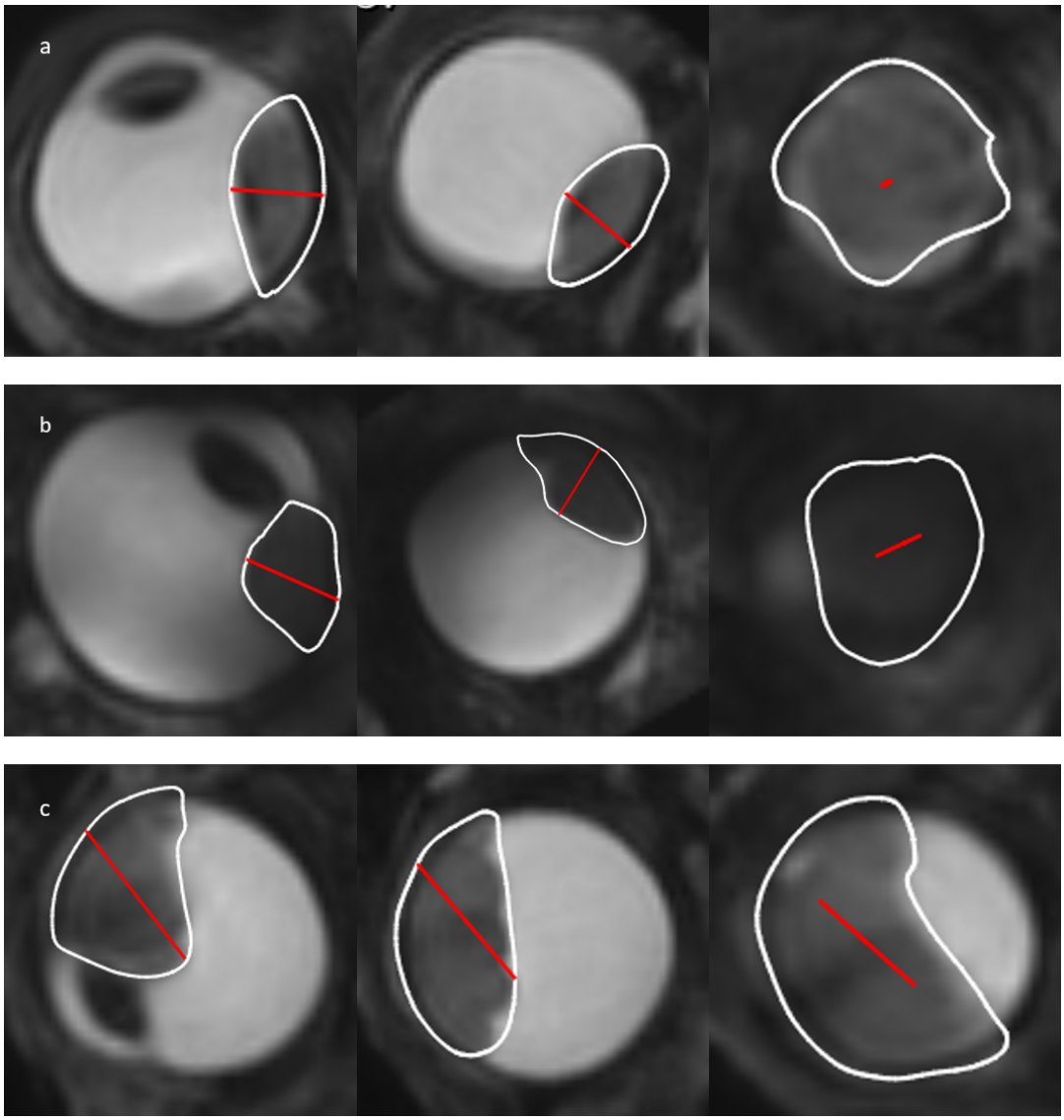

FIGURE 11: (a) example of a clinically acceptable automatic prominence measurement on MRI, (b) example of a debatable automatic prominence measurement on MRI, (c) example of a rejected automatic prominence measurement on MRI.

Appendix 2

	Measurement method 1	Measurement method 2	Significance
Prominence	MRI automatic	MRI manual	0.795
		US	0.930
	MRI manual	MRI automatic	0.795
		US	0.963
	US	MRI auto	0.930
		MRI manual	0.963
LBD	MRI auto	MRI manual	0.059
		US	0.313
	MRI manual	MRI auto	0.059
		US	0.724
	US	MRI auto	0.313
		MRI manual	0.724
SBD	MRI auto	MRI manual	0.960
		US	0.690
	MRI manual	MRI auto	0.960
		US	0.524
	US	MRI auto	0.690
		MRI manual	0.524

TABLE 2: Results of the MANOVA test for the differences in prominence, LBD and SBD across the three measurement methods

Appendix 3

Measurement	Position	n	Mean [mm]	SD [mm]	p
Prominence	Anterior	16	1.08	0.75	0.02*
	Posterior	21	0.58	0.54	
LBD	Anterior	16	1.43	1.78	0.76
	Posterior	21	1.58	1.09	
SBD	Anterior	16	1.79	1.73	0.95
	Posterior	21	1.75	1.15	

TABLE 3: Subgroup analysis for tumour location.
*Significant at $\alpha < 0.05$.